First-principles electronic structure and lattice dynamics of the giant dielectric compound $Na_{0.5}Bi_{0.5}Cu_3Ti_4O_{12}$

2008 J. Phys.: Condens. Matter 20 175220

(http://iopscience.iop.org/0953-8984/20/17/175220)

IOP PUBLISHING JOURNAL OF PHYSICS: CONDENSED MATTER

J. Phys.: Condens. Matter **20** (2008) 175220 (6pp) doi:10.1088/0953-8984/20/17/175220

First-principles electronic structure and lattice dynamics of the giant dielectric compound $Na_{0.5}Bi_{0.5}Cu_3Ti_4O_{12}$

Cihan Parlak and Resul Eryiğit

Department of Physics, Abant Izzet Baysal University, Bolu-14280, Turkey

E-mail: resul@ibu.edu.tr

Received 26 January 2008
Published 7 April 2008
Online at stacks.iop.org/JPhysCM/20/175220

Abstract

We report the results of an *ab initio* study of electronic, dielectric, and lattice dynamical properties of high dielectric constant perovskite-derived oxide $Na_{1/2}Bi_{1/2}Cu_3Ti_4O_{12}$. The calculations have been carried out within the local spin density functional approximation using norm-conserving pseudopotentials and a plane-wave basis. The ground state is found to be an antiferromagnetic direct band gap semiconductor. Lattice dynamical properties, such as Born effective charge tensors, dielectric permittivity tensors, and phonon frequencies at the Brillouin zone center were calculated using density functional perturbation theory and found to be similar to the more studied $CaCu_3Ti_4O_{12}$ and $CdCu_3Ti_4O_{12}$ compounds. The calculated electronic ($\epsilon_\infty \approx 11.5$) and static ($\epsilon_0 \approx 150$) dielectric constants indicate that the observed high dielectric constant is extrinsic in origin. The main contribution to the static dielectric constant is found to be due to a low frequency (50 cm^{-1}) infrared-active mode which has a large mode effective charge.

(Some figures in this article are in colour only in the electronic version)

1. Introduction

Starting with the observation of the giant dielectric constant (GDC) in $CaCu_3Ti_4O_{12}$ (CCTO) [1, 2], perovskite-derived oxides with GDC ($\epsilon_0 > 10^3$) have been the subject of many recent studies, in part because of various potential technological applications of the materials with such properties and in part because of the possible origin of such a high dielectric constant. Investigation of the dielectric properties of many compounds of the form $ACu_3Ti_4O_{12}$, where A might be Ca, Cd, $La_{2/3}$, $Na_{1/2}Y_{1/2}$, or $Na_{1/2}Bi_{1/2}$, showed that all of them had large dielectric constants over a wide temperature range (∼150–600 K) [3, 4]. Ferrarelli *et al* reports room temperature permittivity of over 10 000 for $Na_{1/2}Bi_{1/2}Cu_3Ti_4O_{12}$ (NBCTO) and around 10 000 for CCTO at 100 kHz [3].

Several mechanisms, both extrinsic and intrinsic, have been advanced to shed light on the origin of the giant dielectric response. The proposed intrinsic mechanisms are related to lattice instability that leads to ferroelectric or relaxor-like behavior. Although no ferroelectric phase is observed in GDC compounds [5], Homes *et al* argued that the giant dielectric response might be the result of local dipole moments associated with off-center displacements of Ti atoms [2, 6]. Another intrinsic mechanism is proposed by Ramirez *et al* [7] which focuses on the defects in the Ca–Cu sublattice which might disrupt the Cu–O complex and lead to local polarizability. Recently, Zhu *et al* [8] have shown the existence of a Ca and Cu substitution disorder by using quantitative electron diffraction and extended x-ray absorption fine structure techniques and claimed that the microscopic origin of GDC might be related to this disorder. The proposed extrinsic mechanisms are related to the morphology of the sample and boundary layer effects. Sinclair *et al* attribute the giant dielectric phenomenon to a grain boundary barrier layer capacitance [9, 10] while a number of studies claim a Maxwell–Wagner type source which involves enhancement from the depletion layers at grain boundaries [11, 12].

The first-principles investigation of the electronic, magnetic, and lattice dynamical properties of GDC compounds, mostly CCTO, have been carried out by a number of groups [13–17]. Electronic, magnetic, and lattice dynamical

properties of CCTO and $CdCu_3Ti_4O_{12}$ (CdCTO) were investigated by He *et al* [13, 14] within the ultrasoft pseudopotential local spin density approximation framework [13, 14]. He *et al*'s work focuses on the lattice dynamical properties and the lattice susceptibility contribution to the static dielectric response and found that there was no unstable phonon mode that might lead to a ferroelectric transition and the lattice contribution to the dielectric constant is too low to account for the observed GDC. Electronic and magnetic properties of CCTO were, also, calculated by using the full-potential linearized augmented plane-wave method (FLAPW) within LSDA [15–17]. Li *et al* studied the magnetic structure of CCTO and found that the AFM order is favored over the ferromagnetic and nonmagnetic order. Chen and Wang [18] used a local combination of the atomic orbital basis in the Hartree–Fock (HF) framework to study electronic structure of CCTO and $CaCu_3Mo_40_{12}$ (CCMO) and found that the HF approach was better in determining the energy gap.

The intrinsic bulk permittivity of GDC compounds has also been found to be high compared to the value computed from a simple Clausius–Mossotti relation or density functional calculations by a factor of two for CCTO [13] (experimental value $\sim$ 105) and four (experimental value $\sim$ 235) for NBCTO [3]. Grubbs *et al* have studied the temperature dependent dielectric and magnetic properties of Fe- and Nb-doped CCTO and argued that the intrinsic ϵ' could only be due to a soft polar TO mode [19].

The aim of the present study is to investigate the origin of the dielectric response of $Na_{1/2}Bi_{1/2}Cu_3Ti_4O_{12}$ by using first-principles techniques. To this end we have performed detailed DFT and density functional perturbation theory (DFPT) calculations to determine the electronic structure, magnetization density, and lattice dynamical properties such as Born effective charges and Brillouin zone center phonon frequency and eigenvectors that determine the lattice contribution to the low frequency dielectric constant. The outline of the paper is as follows: in section 2 we give a brief overview of the computational method and the details of the calculational parameters. The calculated structural, electronic, and lattice dynamical properties are presented and discussed in section 3. Section 4 concludes the paper with a brief overview of the main findings of the study.

2. Methodology

All the calculations reported here were done with the Abinit [20] package which is an implementation of density functional theory. Abinit uses plane waves for the expansion of electronic wavefunctions and pseudopotentials for the interaction between electrons and the nuclei. We use the local spin density approximation for the exchange–correlation kernel as parametrized by Perdew and Wang [21]. All atoms are represented by norm-conserving [22] designed nonlocal [23] pseudopotentials which are created by using the OPIUM code [24]. The Na (2s,2p, and 3s), Bi (5d, 6s and 6p), Cu (3d, 4s, and 4p), Ti (3s, 3p, 4s, and 3d), and O (2s and 2p) were treated as valence states. Lattice dynamical and dielectric properties such as Born effective charges,

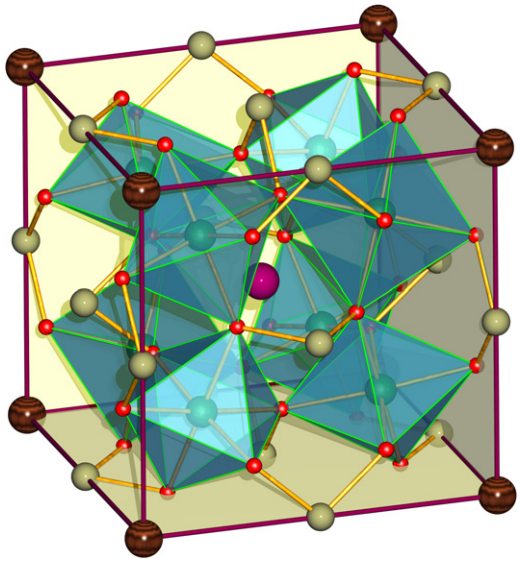

Figure 1. The simple cubic crystal structure of $Na_{1/2}Bi_{1/2}Cu_3Ti_4O_{12}$. The outlined octahedra represent the TiO_6 groups with oxygen at the corners and Ti at the centers. The dark spheres on the corners of the cube represent Na atoms, the gray spheres bonded to the oxygens are Cu atoms and the single sphere at the center of the cube is Bi.

Brillouin zone center phonon frequencies, and oscillator strength are calculated in the linear response formalism of density functional perturbation theory as implemented in Abinit in terms of iterative minimization techniques, which are described by Gonze *et al* in [25, 26]. A plane-wave kinetic energy cutoff of 40 Hartree was found to be enough for the convergence of 1 cm^{-1} in the phonon frequencies. The Brillouin zone integrations were performed with a 444 k-grid.

3. Results and discussion

3.1. Structural properties

The $Na_{1/2}Bi_{1/2}Cu_3Ti_4O_{12}$ crystalline structure, which is shown in figure 1, belongs to the $Pm\bar{3}$ (space group number 200) with Na, Bi, Cu, Ti, and O atoms located at 1a (0,0,0), 1b (1/2, 1/2, 1/2), 3c (1/2, 0, 0), 3d (0, 1/2, 1/2), 8i (x_{Ti}, x_{Ti}, x_{Ti}), 12j (x_{O_1}, y_{O_2}, 0), and 12k (x_{O_2} + 1/2, y_{O_2} + 1/2, 1/2) Wyckoff positions, respectively. The primitive unit cell contains 40 atoms. Minimization of the total energy with respect to the lattice volume gives a lattice constant of 7.375 Å which is in excellent agreement with the measured value of 7.411 Å [3]. The bulk modulus (B_0) and its pressure derivative are calculated as 234 GPa and 4.46, respectively. These values can be compared to the bulk moduli of CCTO (B_0 = 212 ± 2 [27]) and CdCCTO (B_0 = 235 ± 7 [28]). The equilibrium atomic positions are obtained by using the BFGS algorithm, moving the atoms until the maximum force component is less than 0.5 meV $Å^{-1}$. The optimized x_{Ti} is found to be 0.246 which is similar to that of CCTO (x_{Ti} = 0.25 [29]). The x and y parameters of the oxygen positions are found as x_{O_1} = 0.304 and y_{O_1} = 0.179. As the primitive unit cell is rather large, it contains several interesting subcells; the subsystem composed of Na and Bi atoms can be considered

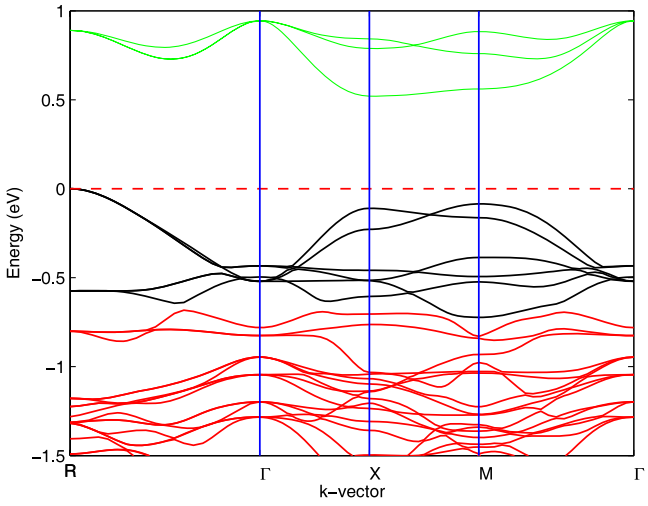

Figure 2. Electronic band structure of $Na_{1/2}Bi_{1/2}Cu_3Ti_4O_{12}$ along the R–Γ–X–M–Γ high symmetry directions of the cubic Brillouin zone.

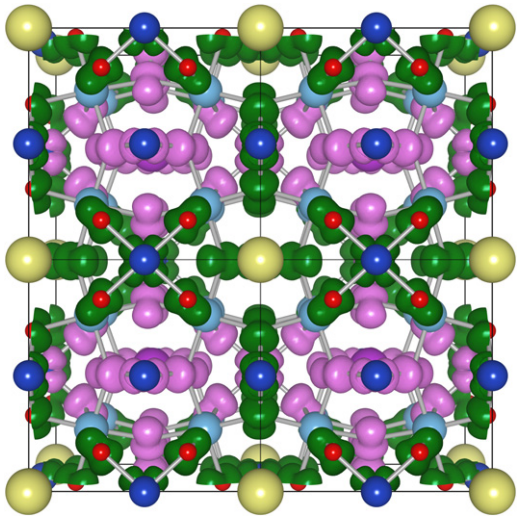

Figure 3. Three-dimensional (3D) isosurfaces of the difference between the up-and down-spin charge densities. Two different values (−0.001 (green/dark) and 0.001 (pink/light) $|e|$) are displayed.

as a large bcc cell with one of them occupying the center of the cell while the other is located at the vertices of the cell. The 40 atom cell contains eight smaller bcc-like cells with the center atom as Ti and vertex atoms as diagonally placed sodium and bismuth and the remaining six vertices occupied by copper atoms. As common with all the other Ti-containing perovskite-derived coasal dielectric materials, Ti cations are placed at the center of oxygen octahedra which are formed by three O_1s and three O_2s. In each one of the octahedra, there exist two types of Ti–O bonds with lengths 1.93 (Ti–O_1) and 1.99 Å (Ti–O_2)(Ti–O bond length in CCTO is 1.96 Å [29]). The TiO_6 octahedron tilting (O–Ti–O angle = 104.05°) is also found to be similar to that in CCTO (104.64°) [29]. Also, Cu_1O_4 and Cu_2O_4 units form planar squares with Cu_1–O_1 = 1.95 Å and Cu_2–O_2 = 1.97 Å. Na and Bi atoms are surrounded by 12 equidistant oxygen atoms. The Na–O distance (2.60 Å) is found to be slightly longer than the Bi–O distance (2.58 Å).

3.2. Electronic structure

The electronic band structure of $Na_{1/2}Bi_{1/2}Cu_3Ti_4O_{12}$ is calculated at the theoretically determined equilibrium geometry and given in figure 2. The non-spin-polarized ground state is found to be metallic with Cu 3d and oxygen 2p derived states forming the bands around the Fermi-level. Including the spin polarization decreases the total energy and leads to an antiferromagnetically ordered semiconducting state with an indirect band gap of 0.53 eV (between R and X points of the cubic BZ). The smallest direct band gap is 0.64 eV at the X point. The calculated band gap is, probably, too low because of a well known deficiency of the local density approximation to the exchange–correlation potential. The observed AFM semiconducting state is similar to the case of a prototype GDC compound CCTO which is known to exhibit an antiferromagnetic transition at ∼25 K [30, 31]. The states near the gap are mostly derived from Cu 3d and O 2p hybridization. The calculated band structure is very similar to that of CCTO reported by [15]. The calculated Hirshfeld charges (Na = 0.11, Bi = 0.55, Cu_1 = 0.44, Cu_2 = 0.42, Ti = 0.24, O_1 = −0.21 and O_2 = −0.22e) indicate that there is net transfer of electrons to oxygen atoms from all the other constituents of the cell. The difference between the up- and down-spin densities, which is a measure of magnetization density, is displayed in figure 3 as isosurfaces for two different values of the difference. Figure 3 clearly reveals the Cu(3d)O(2p) σ-antibonding nature of the magnetic density, which extends over the central cluster composed of a Cu ion and its four close oxygen neighbors at 1.95 and 1.97 Å. This cluster evidently forms a strongly spin-polarized unit with a ferromagnetic alignment of the magnetic moments on the Cu and O atoms comprising it, indicating a significant role of the oxygen atoms in the magnetic structure. From the spin densities copper and oxygen magnetic moments are found to be 0.52 and 0.09 μ_B which are very close to the values reported for the CCTO [13].

3.3. Electronic dielectric tensor and Born effective charges

The Born effective charges, $Z^\star$, describe the change in the macroscopic polarization in response to the displacement of the ions and determine the splitting of the infrared-active optical modes of t he insulating crystals. The calculated $Z^\star$s are presented in table 1 and displayed in figure 4 graphically. The charge imbalance of the cell is found to be less than 0.006e, which is an indication of the quality of convergence of the calculations. The number of nonzero components of the $Z^\star$ tensor for a particular atom depends on the symmetry of the site it occupies in the cell. Na and Bi are located at sites with cubic symmetry T_h and have diagonal $Z^\star$ with equal components. The site symmetry of Cu_1 and Cu_2 is D_{2h} and as a result $Z^\star$(Cu) is diagonal with unequal components. Ti and O are located at lower symmetry sites (C_3 and C_s, respectively) and their effective charge tensors have nonzero, albeit small, off-diagonal components. The difference between $Z^\star(Cu_1)$ and $Z^\star(Cu_2)$ as well as $Z^\star(O_1)$ and $Z^\star(O_2)$ stems from the difference in local structure of

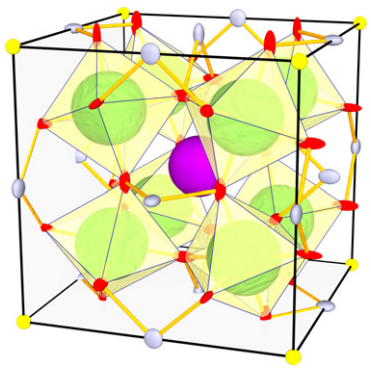

Figure 4. Born effective charges of $Na_{1/2}Bi_{1/2}Cu_3Ti_6O_{12}$. Here each of the atoms is taken as the unit sphere and sheared with its Born effective charge tensor. The placement of the atoms is same as that figure 1.

Table 1. Calculated Born effective charges of $Na_{1/2}Bi_{1/2}Cu_3Ti_4O_{12}$. The eigenvalues, λ, of the symmetric part of $Z^\star$ are given in brackets.

	Effective charge tensor			λ
$Z^\star_{Na}$	Diagonal			[1.20 1.20 1.20]
$Z^\star_{Bi}$	Diagonal			[5.37 5.37 5.37]
$Z^\star_{Cu_1}$	Diagonal			[2.11 2.21 1.15]
$Z^\star_{Cu_2}$	Diagonal			[2.45 1.70 1.19]
$Z^\star_{Ti}$	7.21	0.18	−0.04	[7.13 7.13 7.34]
	−0.04	7.21	0.18	
	0.18	−0.04	7.21	
$Z^\star_{O_1}$	−1.86	0.39	0.00	[−5.57 − 2.39 − 1.39]
	0.60	−1.91	0.00	
	0.00	0.00	−5.58	
$Z^\star_{O_2}$	−2.37	−0.05	0.00	[−4.92 − 2.39 − 2.09]
	0.20	−2.11	0.00	
	0.00	0.00	−4.92	

CuO_4 plaques. The most important observation from table 1 and figure 4 is the anomaly in Ti and O dynamical charges. The large dynamical anomalous charges (compared to the nominal ionic values of Na^{+1}, Bi^{+3}, Cu^{+2}, Ti^{+4} and O^{-2}) originate from the electronic charge reorganization induced when an atom is displaced from its original position. Large values of Born effective charges have been observed in ABO_3 type perovskites and attributed to the hybridization between the occupied O 2p orbital and the unoccupied B 3d orbital [32, 33]. Our calculated Cu, Ti, and O effective charges are similar to those given by He *et al* for CCTO and CdCTO [14]. Also, the principal components of $Z^\star(\mathrm{Ti}) \approx 7.20$ calculated here are comparable to the values reported as 7.16, 7.12, 7.08, and 7.06, in compounds $BaTiO_3$, $SrTiO_3$, $CaTiO_3$, and $PbTiO_3$, respectively [33]. $Z^\star(\mathrm{O})$ are also similar in NBCTO (table 1) and Ti-containing perovskites [33].

The electronic part of the dielectric tensor is isotropic (as expected from the cubic T_h point group symmetry) with a value $\epsilon_\infty = 11.8$. There is no experimental value of ϵ_∞ to compare but it is well known that the LDA overestimates the ϵ_∞ because of the band gap problem.

Table 2. TO frequencies (in cm^{-1}), mode effective charges (in $|e|$), and the mode contribution to the static dielectric constant of IR-active zone center phonons of $Na_{1/2}Bi_{1/2}Cu_3Ti_6O_{12}$.

ω_i	Z^*_i	$\Delta\epsilon_i$	ω_i	Z^*_i	$\Delta\epsilon_i$
50	9.59	63.78	295	1.86	0.28
108	10.57	25.41	335	1.98	0.32
126	3.72	1.81	381	7.45	1.36
142	9.51	15.05	406	12.41	3.37
146	3.95	2.50	436	9.25	2.55
177	5.81	4.60	492	4.62	0.36
184	4.63	2.33	496	1.96	0.10
206	1.61	0.21	533	0.53	0.00
236	11.14	13.52	540	2.63	0.17
268	1.98	0.37	682	2.94	0.14

3.4. Zone center phonon frequencies and static dielectric constant

The primitive unit cell contains 40 atoms which leads to a total of 120 phonon modes which can be decomposed into the following sum of irreducible representations [34]:

$$\Gamma = 5A_g \oplus 5E_g \oplus 11T_g \oplus 3A_u \oplus 3E_u \oplus 21T_u.$$

Among these phonon modes, only T_{1u} are IR-active, A_g, E_g and T_g are Raman-active. A_u and E_u modes are optically silent.

We will present the properties of phonons in two groups based on the activities of the modes. The first group is comprised of 21 T_u modes which are IR-active. IR-active modes determine the lattice susceptibility contribution to the static dielectric constant and it is known that for most of the insulating perovskites [35] and the CCTO [13] the lattice contribution to ϵ_0 is much higher than the electronic one. One of the triply degenerate T_u symmetry modes forms the acoustic branch with zero frequency. Frequency, mode effective charge, and oscillator strength of the remaining 20 T_u modes are presented in table 2. Since, to the best of our knowledge, there are no experimental data on phonons of NBCTO, we will compare the calculated quantities with experimental and computational data of CCTO and CdCTO. The most important finding here is the existence of a very low frequency polar mode at 50 cm^{-1} which has a large mode effective charge. The eigen-displacement of this low frequency T_u mode is displayed graphically in figure 5(a) and involves the anti-parallel motion of Na and Bi as a group against the Cu and O atoms. The displacement pattern of Ti atoms is a breathing type motion with much smaller amplitude compared to the displacement of the other atoms. The low frequency T_u mode was found to be important in possible explanations of the relatively high low-temperature intrinsic dielectric constant of CCTO. Homes *et al* [2] have found that its frequency decreases while the oscillator strength of it increases with an f-sum rule violation. The frequency of this mode was found at 125 and 72 cm^{-1} for CCTO and CdCTO by He *et al* and $\omega = 50$ cm^{-1} calculated here seems to indicate that it is proportional to the inverse square root of the mass of Ca, Cd, and Bi in the three compounds. The remaining T_u mode frequencies range from 108 to 682 cm^{-1}. The lattice contribution to the static dielectric

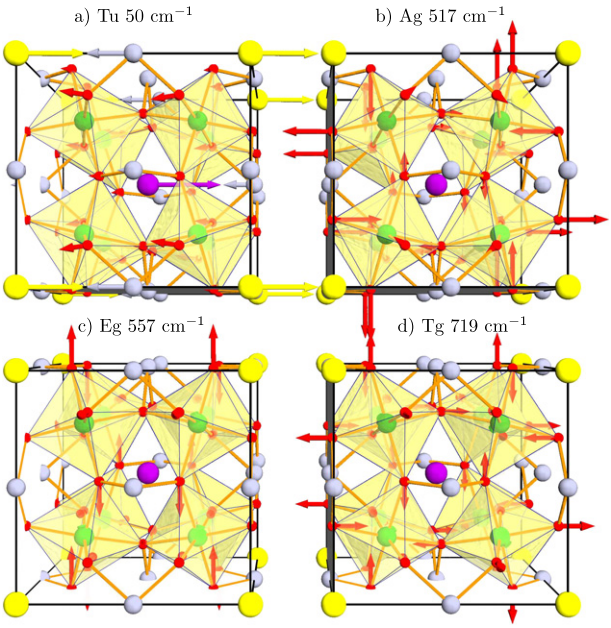

Figure 5. Eigen-displacement patterns of (a) the lowest frequency T_u,and the highest frequency (b) A_g, (c) E_g, and (d) T_g modes.

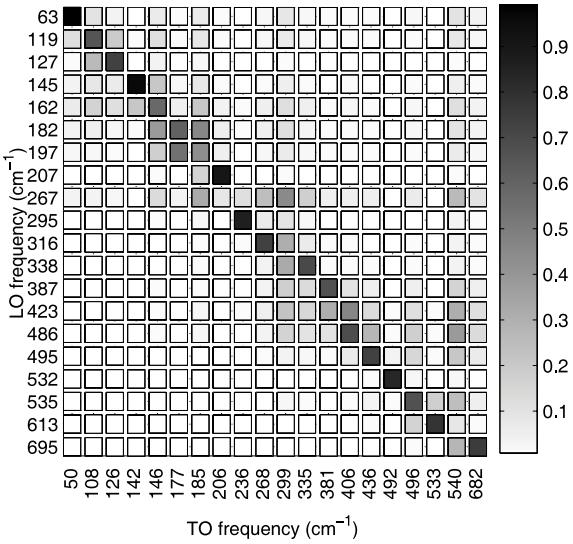

Figure 6. LO–TO overlaps of the IR-active modes.

Table 3. Nonpolar phonon mode frequencies (cm^{-1}).

Mode symmetry											
A_g	295	409	459	464	517						
E_g	272	308	378	533	557						
T_g	105	125	180	267	295	388	430	434	481	518	719
A_u	145	415	753								
E_u	103	436	514								

constant of the modes given in table 2 is around 138 (the highest contributions being from the modes at 50 ($\Delta\epsilon_i$ = 63.78), 108 ($\Delta\epsilon_i$ = 25.41), 142 ($\Delta\epsilon_i$ = 15.05), and 236 ($\Delta\epsilon_i$ = 13.52) cm^{-1}). Although the mode at 406 cm^{-1} has the largest mode effective charge, its contribution to the dielectric constant is low because the contribution is inversely proportional to the square of the mode frequency. The low frequency polar modes with high mode effective charges might explain the high intrinsic dielectric constant of 235 reported by Ferrarelli *et al* [3] for NBCTO. The relatively low values of the minimum optical frequencies in NBCTO are partly related to the high mass of bismuth. Modes with frequencies larger than 200 cm^{-1} involve, mostly, the motion of Cu and O atoms while all the atoms partake in the lower frequency modes. Comparing our calculated high frequency T_u modes with those of CCTO and CdCTO [14], one can see that the effect of cation A is minimal in the determination of frequencies of these modes; this finding is expected because the mode patterns of these modes involve motion of Cu, Ti, and O atoms only. It seems relatively safe to argue that the high intrinsic static dielectric constant observed in GDCs is related to the anomalous Born effective charges which is common for Ti–O octahedral structure and the low frequency polar phonon mode whose frequency inversely scales with the square root of the cation mass.

An interesting observation concerning the effect of the Coulomb interaction on the polar modes of perovskite ferroelectrics is the giant LO–TO splitting of the IR-active polar modes [33]. An investigation of the overlap matrix of mass matrix $M_{mn} = M_m\delta_{mn}$ between the LO and TO mode eigenvectors as $c_{ij} = \langle\xi_i^{TO}|M|\xi_j^{LO}\rangle$ was carried out and the overlap matrix for NBCTO is given in figure 6. Although some of the TO modes (at 185, 299, and 540 cm^{-1}) have appreciable overlap with more than one LO mode, there is no giant splitting in any of the modes. The largest LO–TO splitting is found for the TO mode at 533 cm^{-1} which has a corresponding LO frequency of 613 cm^{-1}.

The frequencies of Raman-active and silent modes are given in table 3. The Raman-active modes can be broadly divided into four groups based on the magnitude of the vibration frequency as follows: a low frequency group of modes with T_g symmetry and $\nu \approx$ 105 and 180 cm^{-1}, a group of modes in the $\nu \approx$ 267 and 308 cm^{-1} range (one from each one of the symmetries), a total of 11 modes in the 378–557 cm^{-1} range, and finally the highest frequency T_g mode at 719 cm^{-1}, which is comparable to 739 cm^{-1} reported for the highest frequency T_g mode for CCTO [13]. Modes of T_g symmetry mainly consist of collective TiO_6 octahedral rotational or octahedral breathing type displacements. The calculated highest frequency A_g and E_g and T_g modes at 517, 557, and 719 cm^{-1}, respectively, are similar to those reported for CCTO at 519, 568, and 729 cm^{-1}. The eigen-displacement patterns of the highest frequency A_g, E_g, and T_g modes are displayed in figures 5(b), (c), and (d) respectively. All of the Raman-active modes shown in figure 5 involve, mostly, various breathing type motions of oxygen octahedra. The displacements of Ti atoms are of clockwise or anticlockwise rotation type with much smaller amplitude compared to those of the oxygens.

4. Conclusions

We have investigated the structural, electronic, and lattice dynamical properties of the high dielectric compound $Na_{1/2}Bi_{1/2}Cu_3Ti_6O_{12}$ in the DFT framework. The main features of the structure are found to be tilted TiO_6 octahedra, planar square CuO_4 units, and 12-coordinated NaO_{12} and BiO_{12} icosohedra. The compound is found to be an antiferromagnetic insulator with an indirect band gap of 0.65 eV. The electronic structure near the valence band maximum and conduction band minimum is found to originate mainly from the hybridization of copper 3d and oxygen 2p states, as is common in many compounds that contain CuO_4 planar structures. The magnetic moments of Cu and O atoms are found to be 0.52 μ_B and 0.09 μ_B, respectively. These values are similar to those reported for the other GDCs.

The dynamical Born effective charges were found to be close to nominal values of Na (nominal +1 versus $Z^\star = 1.20$), Bi (nominal +3 versus $Z^\star = 5.47$), and Cu (nominal +2 versus $Z^\star_{av} = 1.90$) atoms, while the $Z^\star$ of Ti and O atoms are anomalous, with components as large as 7.21 for Ti and −5.58 for the oxygen. The lattice contribution to the static dielectric constant is calculated to be ≈138 which is mostly due to the four IR-active modes with frequency less than236 cm^{-1}. The total static dielectric constant, $\epsilon_\infty \approx 150$ is much smaller than the experimentally reported value of 3400 above 100 K, but close to the low-temperature value of 235. This finding suggests that the origin of the coasal ϵ reported for $Na_{1/2}Bi_{1/2}Cu_3Ti_6O_{12}$ is, also, extrinsic.

Acknowledgments

This work was supported by Tübitak under grant no. TBAG-2449(104T057) and AIBU Research Fund grant no. 04.03.02.199.

References

[1] Subramanian M A, Li D, Reisner B A and Sleight A W 2000 *J. Solid State Chem.* **151** 323
[2] Homes C C, Vogt T, Shapiro S M, Wakimoto S and Ramirez A P 2001 *Science* **293** 673
[3] Ferrarelli M C, Adams T B, Feteira A, Sinclair D C and West A R 2006 *Appl. Phys. Lett.* **89** 212904
[4] Subramanian M A and Sleight A W 2002 *Solid State Sci.* **4** 347
[5] Ramirez A P, Subramanian M A, Gardel M, Blumberg G, Li D, Vogt T and Shapiro S M 2000 *Solid State Commun.* **115** 217
[6] Liu Y, Withers R L and Wei X Y 2005 *Phys. Rev.* B **72** 134104
[7] Ramirez A P, Lawes G, Butko V, Subramanian M A and Varma C M 2002 *Preprint* cond-mat/0209498
[8] Zhu Y, Zheng J C, Wu L, Frenkel A I, Hanson J, Northrup P and Ku W 2007 *Phys. Rev. Lett.* **99** 037602
[9] Sinclair D C, Adams T B, Morrison F D and West A R 2002 *Appl. Phys. Lett.* **80** 2153
[10] Cohen M H, Neaton J B, He L and Vanderbilt D 2003 *Preprint* cond-mat/0304196
[11] Lunkenheimer P, Bobnar V, Pronin A V, Ritus A I, Volkov A A and Loidl A 2002 *Phys. Rev.* B **66** 052105
[12] Lunkenheimer P, Fichtl R, Ebbinghaus S G and Loidl A 2004 *Phys. Rev.* B **70** 172102
[13] He L, Neaton J B, Cohen M H, Vanderbilt D and Homes C C 2002 *Phys. Rev.* B **65** 214112
[14] He L, Neaton J B, Vanderbilt D and Cohen M H 2003 *Phys. Rev.* B **67** 012103
[15] Li G-L, Yin Z and Zhang M-S 2005 *Phys. Lett.* A **344** 238
[16] Weht R and Pickett W E 2001 *Phys. Rev.* B **65** 014415
[17] Johannes M D, Pickett W E and Weht R 2002 *Mater. Res. Soc. Symp. Proc.* **718** 25
[18] Chen L and Wang C L 2007 *J. Mag. Mag. Mater.* **312** 266
[19] Grubbs R K, Venturini E L, Clem P G, Richardson J J, Tuttle B A and Samara G A 2005 *Phys. Rev.* B **72** 104111
[20] The ABINIT code is a common project of the Universite Catholique de Louvain, Corning Incorporated, and other contributors (www.abinit.org); see Gonze X, Beuken J-M, Caracas R, Detraux F, Fuchs M, Rignanese G-M, Sindic L, Verstraete M, Zerah G, Jollet F, Torrent M, Roy A, Mikami M, Ghosez Ph, Raty J-Y and Allan D C 2002 *Comput. Mater. Sci.* **25** 478
[21] Perdew J P and Wang Y 1992 *Phys. Rev.* B **45** 13 244
[22] Rappe A M, Rabe K M, Kaxiras E and Joannopoulos J D 1990 *Phys. Rev.* B **41** 1227
[23] Ramer N J and Rappe A M 1999 *Phys. Rev.* B **59** 12471
[24] http://opium.sourceforge.net
[25] Gonze X 1997 *Phys. Rev.* B **55** 10337
[26] Gonze X and Lee C 1997 *Phys. Rev.* B **55** 10355
[27] Valim D, Souza Filho A G, Freire P T C, Fagan S B, Ayala A P, Filho J M, Almeida A F L, Fechine P B A, Sombra A S B, Staun Olsen J and Gerward L 2004 *Phys. Rev.* B **70** 132103
[28] Yanzhang Ma and Aksoy R 2007 *Solid State Commun.* **142** 376
[29] Fagan S B, Souza Filho A G, Ayala A P and Mendes Filho J 2005 *Phys. Rev.* B **72** 014106
[30] Koitzsch A, Blumberg G, Gozar A, Dennis B, Ramirez A P, Trebst S and Wakimoto S 2002 *Phys. Rev.* B **65** 052406
[31] Mozzati M C, Azzoni C B, Capsoni D, Bini M and Massarotti V 2003 *J. Phys.: Condens. Matter* **15** 7365
[32] Ghosez Ph, Michenaud J-P and Gonze X 1998 *Phys. Rev.* B **58** 6224
[33] Zhong W, King-Smith R D and Vanderbilt D 1994 *Phys. Rev. Lett.* **72** 3618
[34] Kroumova E, Aroyo M I, Perez Mato J M, Kirov A, Capillas C, Ivantchev S and Wondratschek H 2003 *Phase Transit.* **76** 155
[35] Cockayne E and Burton B P 2000 *Phys. Rev.* B **62** 3735